A validation study of the flamelet approach's ability to predict flame structure when fluid mechanics are fully resolved

By E. Knudsen AND H. Pitsch

1. Motivation and objective

Modern combustion devices are designed to balance the need for efficient performance with the need for robust performance. Presently available design techniques are capable of meaningfully informing how this balance should be struck. To truly optimize the efficiency and robustness of a combustor, however, the predictive capabilities of numerical simulations will have to be more heavily relied upon. This is because the variables that describe the multi-dimensional combustor design space are related in highly non-linear ways. While empirical numerical models that depict transitions between burned and unburned states are readily available, these models do not provide the level of detail needed for optimizing a combustor's efficiency. For example, the evolution of important quantities such as CO, NO_X, and soot often depend on the details of the time and spatial scales that characterize the structure of the reaction zone.

Flamelet approaches are a particular class of combustion model that do capture the time and spatial scales associated with a given asymptotic limit of combustion physics (Peters 2000; Pierce & Moin 2004; Pitsch 2006). This ability to capture the correct limiting physics has historically been viewed as the advantage of the flamelet approach. In modern combustors where mixed-regime behavior is expected, however, the applicability limits of the flamelet approach are not yet well bounded. Single regime non-premixed flamelet implementations, for instance, would not be expected to accurately describe partially premixed or unsteady combustion processes. Furthermore, because the sensitivity of CO, NO_X, and soot to predicted reaction zone structure is not fully understood, the accuracy with which single- or multi-regime flamelet approaches predict pollutants in realistic combustors is not known. Therefore it is not currently possible to perform the kind of cost and benefit analysis that is important in selecting an appropriate combustion model for a given application.

The objective of this study is to analyze how accurately current flamelet approaches describe complex reaction zone structure in a fully resolved, multi-regime, multi-dimensional laminar flame. Two questions will be used to target this objective. First, how well do single regime (non-premixed) flamelet approaches simulate the detailed flame structure and pollutant signature? Second, do recently developed implementations of multi-regime flamelet methods capture flame structures in any more detail? These questions will be answered by using the flamelet approach to model an unsteady laminar triple flame that has been simulated using a finite rate chemical mechanism for n-heptane.

2. Triple flame simulation

A laminar triple flame similar to one originally studied by Favier and Vervisch (Favier & Vervisch 2001) and later considered by Knudsen and Pitsch (Knudsen & Pitsch 2009*a*)

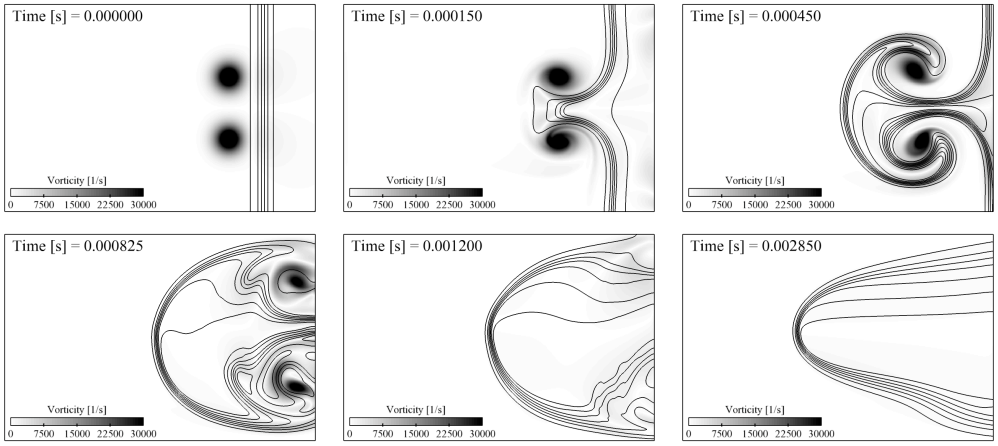

FIGURE 1. Time series of the finite rate triple flame simulation. The contour plots depict vorticity while the lines depict isocontours of the progress variable field.

is used as a validation case. This flame simulation is initialized by placing two counter-rotating vortices in the middle of a 9 mm $\times$ 6 mm two-dimensional domain. Behind these vorticies, a progress variable profile with a hyperbolic tangent profile is introduced. A tabulated set of premixed flamelet solutions, described in more detail below, is then accessed to set the values of the individual chemical species and temperature throughout this profile. The inlet of the simulation, which consists of the entire left side of the domain, is set to have a constant bulk value of downstream velocity and zero cross-stream velocity. The species and temperature profiles along this inlet are set to fully unburned values, but a mixture fraction gradient is created in the cross-stream direction along the inlet so that the effects of both premixed and non-premixed combustion can be considered. The outlet boundary conditions, on the opposite side of the domain, are solved by using a convective equation. The boundaries at the top and bottom of the domain are set as slip walls. The simulation is run until the influence of the vortices has disappeared and a steady, propagating triple flame has formed. A time series of the progress variable field from the simulation is shown in Fig. 1.

2.1. *Flow solver and chemical mechanism*

The triple flame is simulated using a structured finite-difference code (Desjardins *et al.* 2007) that solves the Navier-Stokes and scalar transport equations in the low Mach number limit. The code is run using implicit time-stepping, and a spatially second-order accurate scheme is used to evaluate velocity and pressure gradients. A third-order accurate WENO scheme is used to evaluate scalar gradients. For the baseline finite rate chemistry case, chemical source terms are integrated between timesteps at each point in the flow using the implicit integration package DVODE. The mesh for this simulation consists of 384 $\times$ 256 points, is uniform and Cartesian, and resolves reaction layers on approximately 9 points.

A reduced n-heptane mechanism (Liu *et al.* 2004) is used to describe chemical kinetics in all of the finite rate chemistry and flamelet calculations that are performed. This reduced mechanism requires solving transport equations for 20 species, and an additional 24 species are algebraically solved for by employing the assumption that they are in steady state. Unity Lewis numbers are used for all calculations in this study, but the effects of

non-unity Lewis numbers will be considered in future work. A progress variable will be defined for this mechanism as $C = Y_{H_2O} + Y_{H_2} + Y_{CO} + Y_{CO_2}$. The mixture fraction will be defined as having a value of 1.0 in a stream consisting of pure n-heptane, and a value of 0.0 in a stream consisting of pure air. Note that the maximum value of mixture fraction that is injected at the triple flame simulation inlet is $Z = 0.5$, rather than $Z = 1.0$. The mixture fraction gradient at the inlet therefore prescribes a change between 0.5 and 0.0 in Z-space.

2.2. *Flamelet modeling approach*

2.2.1. *Single regime non-premixed flamelet model*

In an effort to better understand how accurately flamelet models predict the evolution of flame structure in mixed-regime settings, the triple flame will also be simulated using several flamelet model implementations. The first model considered is the so-called Flamelet Progress Variable (FPV) approach (Ihme *et al.* 2004; Pierce & Moin 2004). In this approach, the steady non-premixed flamelet equations,

$$0 = \rho \frac{\chi_Z}{2} \frac{\partial^2}{\partial Z^2}(\phi_i) + \rho \dot{\omega}_i, \tag{2.1}$$

are solved for each chemical species i in a mechanism. The scalar dissipation rate $\chi_Z = 2\mathcal{D}(\nabla Z \cdot \nabla Z)$ that appears in Eq. (2.1) is modeled as a prescribed function of Z, with the maximum value of χ_Z serving as a parameter that is external to the system (Peters 2000; Pitsch & Peters 1998). It is interesting to note that the functional form of the χ_Z model used here decays to zero only when $Z = 0$ or $Z = 1$. In the triple flame, however, χ_Z always decays to zero at the point where $Z = 0.5$, because that is the maximum value of the mixture fraction in the simulation. Rather than adjusting the definition of mixture fraction or the form of the χ_Z model to compensate for this effect, the model is tested as-is. In keeping with the objective of this study, such a test will measure the flamelet model's ability to describe combustion in the kind of mixed regime encountered in modern combustors. For example, in a partially premixed setting a pocket of gas where $Z = 0.5$ could form and exist in an unburned state, even though the combustor inlet stream is characterized by the value $Z = 1.0$.

The non-premixed flamelet equations, Eqs. (2.1), are solved for the relevant n-heptane mechanism using the FlameMaster program (Pitsch 1998). In accordance with the FPV approach, these solutions are then tabulated and stored in a database as a function of the mixture fraction Z and progress variable C. Because the fluid mechanics in the triple flame simulation are fully resolved, no turbulence modeling or integration against presumed PDFs is required. The simulation therefore isolates the accuracy of the flamelet approach.

Three different sets of flamelets will be considered for use in the flamelet database that is needed in the non-premixed FPV approach. The non-premixed flamelet sets that will be sampled from are shown in Fig. 2, where the temperature solution from each of the flamelets is plotted as a function of the mixture fraction Z. As an addendum to the discussion of the modeled scalar dissipation rate χ_Z, it is interesting to note that setting $\chi_Z = 0 \ \forall \ Z > 0.5$ in Fig. 2 would eliminate the curvature in the flamelet solutions above $Z = 0.5$. This region of flamelet space is never accessed in the triple flame simulation, but the associated change in diffusion processes would perturb the flamelet solutions on the rich side of the stoichiometric mixture fraction, $Z_{st} = 0.062$. The extent to which this modeling choice induces errors in the flamelet predictions can be seen in the results section below.

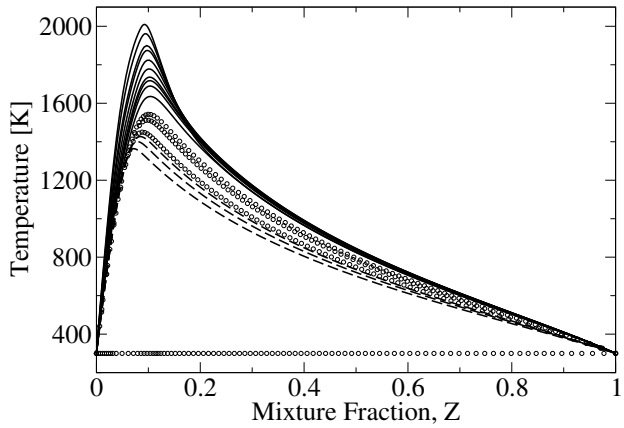

FIGURE 2. The steady non-premixed flamelets used to create the three non-premixed chemistry tables. Flamelet Set #1 (——); Flamelet Set #2 (○ ○ ○); Flamelet Set #3 (– – –).

The first flamelet table that is created for use in the FPV model is based on Flamelet Set #1 from Fig. 2. This set consists only of burning flamelets, and therefore unburned reactants are only permitted to exist around $Z = 0$ and $Z = 1$. When the table is accessed using a mixture fraction and progress variable that exist outside the bounds of these burning flamelets, it returns a quantity from the nearest flamelet in (Z,C) space. The one exception to this is the progress variable source term, which is set to zero outside of the realizable flamelet bounds.

The second flamelet table that is created makes use of the flamelets from both Flamelet Set #1 and Flamelet Set #2. Flamelet Set #2 consists of an unburning solution ($T = 300$ K $\forall\ Z$) and several solutions near the turning point of the so-called S-shaped curve (Ihme *et al.* 2004; Peters 2000). The solutions near the turning point in Set #2 are still burning reasonably strongly, and this affects the progress variable source terms that the tabulated database returns when the progress variable itself sits between the burning and non-burning solutions. For progress variable values that characterize the space between the burning solution with the lowest temperature and the non-burning solution, the table is accessed by interpolating between these two nearest flamelets. Because the middle branch flamelets in Flamelet Set #2 have reasonably large source terms, this interpolation will produce small but non-zero source terms for small values of the progress variable C.

The third and final non-premixed table that will be developed adds Flamelet Set #3 to the first two sets. This third table therefore contains information from all of the flamelets that are shown in Fig. 2. The flamelets in Set #3 are burning much more weakly than those in set #2, and so interpolations between the non-burning and the most weakly burning solutions yield negligible values of the progress variable source term in the third table. Including Set #3 in the flamelet database effectively ensures that the fullest possible range of scalar dissipation rates χ_Z are included in the steady table. The effect associated with each of the three different flamelet sets will be examined in more detail in the results section below.

Once the non-premixed flamelet tables are created, the FPV model is applied by solving transport equations for the mixture fraction Z and the progress variable C. A tabulated flamelet database is then accessed to locally determine a quantity ϕ_i as $\phi_i = \phi_i(Z, C)$. The ϕ_i may represent density, temperature, or any chemical species.

2.2.2. *Multi-regime premixed and non-premixed flamelet model*

Although non-premixed flamelets can be used to model partially premixed or lifted flame physics, it is clear that they will have difficulty accounting for the purely premixed regime. Furthermore, the accuracy with which they can single handedly account for partially premixed combustion is unclear. Accordingly, recent developments in flamelet modeling have moved in the direction of multi-regime approaches where non-premixed, premixed, and auto-ignition tabulated databases are used concurrently in a flow (Domingo *et al.* 2005, 2008; Knudsen & Pitsch 2009*a*). To analyze the accuracy of these multi-regime approaches, a combined premixed and non-premixed flamelet model will be tested as a second baseline model for the triple flame simulation.

This multi-regime approach follows prior work (Knudsen & Pitsch 2009*a*,*b*) in which both premixed and non-premixed tabulated databases are created and used for mapping reacting quantities into a flow field. To set up such a multi-regime model for the triple flame simulation, FlameMaster is again applied to the n-heptane mechanism to solve the steady unstretched premixed flamelet equations,

$$\rho_u \mathrm{s}_{L,u} \frac{d}{dx}(\phi_i) = \frac{d}{dx}\left(\rho \mathcal{D}_i \frac{d}{dx}(\phi_i)\right) + \rho \dot{\omega}_i, \tag{2.2}$$

where $\mathrm{s}_{L,u}$ is the laminar flame speed. The premixed solution sets are tabulated as a function of the mixture fraction Z (the equivalence ratio) and the progress variable C. Non-premixed and premixed tabulated databases of the form $\phi_i = \phi_{i,np}(Z,C)$ and $\phi_i = \phi_{i,p}(Z,C)$ are then available for use in the triple flame simulation.

A method of selecting the combustion regime is needed in order to determine which of these tables to locally and instantaneously access. One such method is the flame index (Domingo *et al.* 2005; Yamashita *et al.* 1996), but here a combustion regime index (Knudsen & Pitsch 2009*a*) will be used that explicitly accounts for the relative importance of the timescales associated with each regime. This combustion regime index can be written using a flamelet parameter Λ that describes the temperature of a non-premixed flamelet at a particular value of Z. A single Λ value is associated with a single steady non-premixed flamelet, and Λ is therefore statistically independent of the mixture fraction in a given flamelet. The combustion regime index leverages this statistical independence to compare the terms that balance the chemical source term $\dot{\omega}_i$ from Eqs. (2.1) and (2.2) in these premixed and non-premixed limiting cases. If the progress variable is selected as the scalar ϕ_i, the combustion regime index Θ may be written (Knudsen & Pitsch 2009*a*)

$$\Theta_{num} = \partial_\Lambda C \left[\rho_u s_{L,u} \left|\nabla \Lambda\right| - \nabla \cdot (\rho \mathcal{D} \nabla \Lambda)\right], \tag{2.3}$$

$$\Theta_{den} = -\rho \frac{\chi_Z}{2} \partial_Z^2 C, \tag{2.4}$$

$$\Theta = \frac{\Theta_{num}}{\Theta_{den}}, \tag{2.5}$$

where the numerator describes how the source term is balanced in the premixed limit and the denominator describes how the source term is balanced in the non-premixed limit. When $\Theta \ll 1$, the non-premixed regime characterizes combustion. Conversely, the premixed regime characterizes combustion when $\Theta \gg 1$. It is important to note that the quantities Λ, $\partial_\Lambda C$, and $\partial_Z^2 C$, are not immediately available from transport equations, and so must be called from a table.

The issue of how to select between the $\phi_{i,np}(Z,C)$ and $\phi_{i,p}(Z,C)$ solutions for a given value of Θ is an open research question. In the simulations presented here, the magnitude

of the index Θ will be used to blend these solutions according to the rule

$$\phi_i(\xi, Z, C) = \phi_{i,np}(Z, C) \cdot (1 - \xi) + \phi_{i,p}(Z, C) \cdot \xi, \tag{2.6}$$

where

$$\xi = \frac{\Theta_{num}}{\max(\Theta_{num} + \Theta_{den}, \epsilon)}, \tag{2.7}$$

and ϵ is a small, positive number. The limiting cases of fully premixed and fully non-premixed combustion are captured by this blending, where $\xi \to 1$ when $\Theta_{num} \gg \Theta_{den}$, and conversely $\xi \to 0$ when $\Theta_{den} \gg \Theta_{num}$.

Two different multi-regime flamelet implementations will be tested. Just as in the non-premixed FPV approach, scalar transport equations for Z and C will be solved in both of these multi-regime tests. In the first implementation, the C-equation is solved for without using any special numerical techniques. Such an unmodified progress variable equation could not be used in an LES, however, due to the numerical errors that would occur around the sharp jump in C that exists at the flame front (Colin *et al.* 2000; Moureau *et al.* 2009). In the second implementation, therefore, a level set description of the flame front is introduced and the C equation is coupled to it through the progress variable source term. In the vicinity of the flame front this coupling is enforced by accessing tabulated C source terms based on the level set rather than the transported C value. Further details of this coupling are described elsewhere (Knudsen & Pitsch 2009*b*). In the present context it is sufficient to simply emphasize that the level set coupling is a realizable LES approach.

3. Results

In this section the triple flame simulations associated with each of the models from section 2 are presented and compared with the finite rate solution. This results section focuses on predictions of the progress variable C, the density ρ, and the chemical species CO. The CO species is considered because of its ability, as a minor species in the detailed mechanism, to describe whether flame structure has been correctly captured by the flamelet models.

3.1. *Non-premixed FPV approach; burning flamelets only*

The first FPV implementation is based solely on information from Flamelet Set #1 in Fig. 2. As such, no flamelet in the model describes the cold mixing line connecting the $Z = 0$ and $Z = 1$ boundary conditions. Although the marginal computational costs associated with including a non-burning flamelet (such as from Flamelet Set #2) in a chemistry database are virtually non-existent, flamelets that are all fully burning are still sometimes used to create databases for simulations and analysis. The decision to neglect non-burning or weakly burning solutions is often made either to simplify the approach, or to reduce the numerical difficulties that sometimes arise when flamelets are stored and accessed from a table.

As expected, tests of the first FPV model showed that mapping burning flamelet solutions into the entire triple flame simulation domain severely differentiated the model from the finite rate chemistry case. Because of this mapping, the model was unable to distinguish between the burning and the non-burning regions of the flow. The density and progress variable fields were therefore incorrect throughout large regions of the modeled flow field.

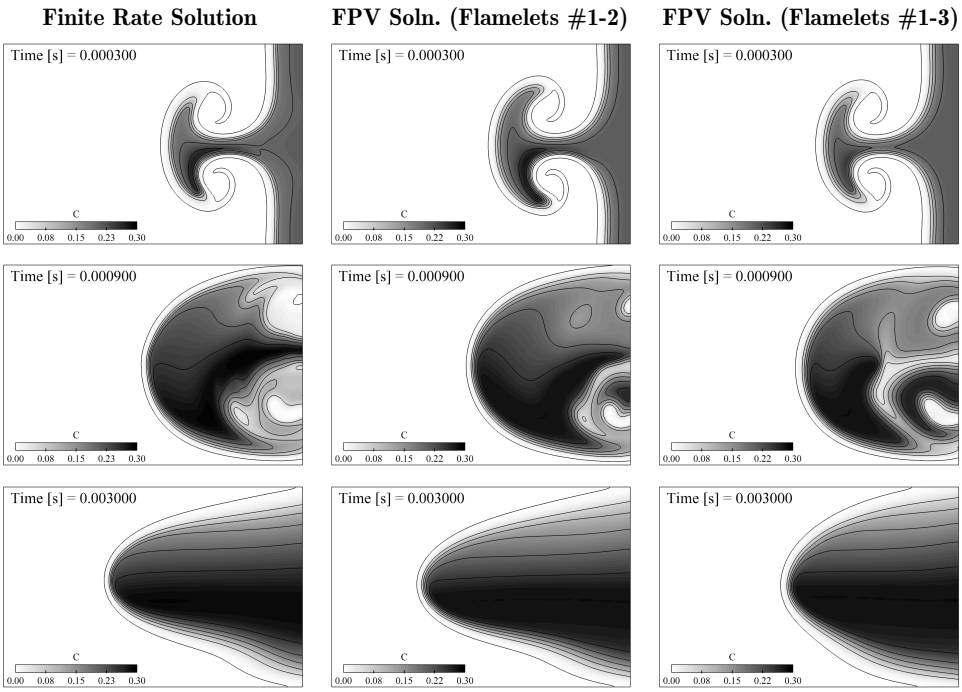

FIGURE 3. Progress variable fields in the triple flame, computed from the finite rate approach and from two non-premixed FPV models. The models use Flamelet Sets #1-2 and #1-3 from Fig. 2.

Because of its inability to describe the basic dynamics of the triple flame, this first FPV implementation can be labeled as the least accurate of all the flamelet models being considered. Images from the tests of this model are not shown, but they confirmed that the premixing inherent in the triple flame flow field caused this first implementation of the FPV model to fail.

3.2. *Non-premixed FPV approach; non-burning flamelet included*

The second and third non-premixed FPV implementations are compared with the finite rate solution in Figs. 3 and 4. The second FPV implementation uses Flamelet Sets #1 and #2 from Fig. 2; the third implementation uses Sets #1, #2, and #3. These models tend to agree with the finite rate solution much better than the first fully burning FPV implementation, but they still differ from the 'true' finite rate solution in important ways.

The inclusion of a non-burning flamelet in both the second and third implementations allows these models to differentiate between burned and unburned gases. Accordingly, the models tend to predict the location of the flame front with moderate accuracy. Interestingly, Fig. 3 demonstrates that including the weakly burning flamelets from Set #3 especially affects the appearance of the flame front at the last point in time that is considered (the bottom row of Fig. 3). The flame front in the third implementation somewhat lags the finite rate flame front, and is characterized by a shape that is relatively broader and more rounded. This effect on the front occurs because the source terms in the weakly burning Flamelet Set #3 are very small. These small source terms are accessed in the leading edge of the flame and cause it to propagate at a reduced speed relative to both the second FPV implementation and the finite rate solution (see

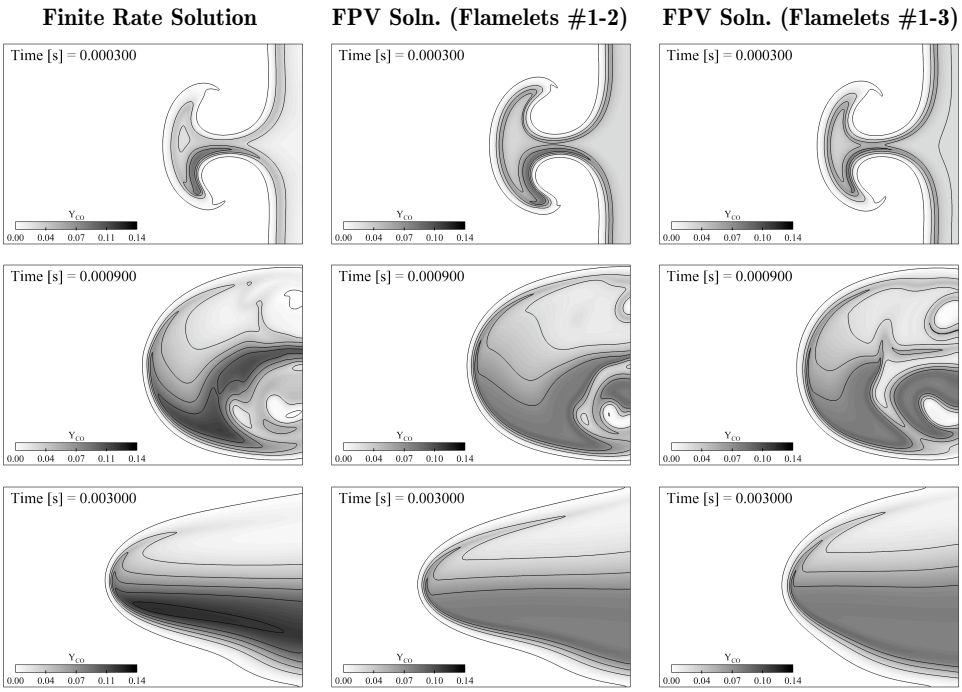

FIGURE 4. CO fields in the triple flame, computed from the finite rate approach and from two non-premixed FPV models. The models use Flamelet Sets #1-2 and #1-3 from Fig. 2.

Fig. 8 below). Conversely, the implementation that uses Flamelet Sets #1 and #2 tends to propagate at a speed that is somewhat too high (see Fig. 8). At relatively small values of the progress variable this second implementation generates a source term by interpolating between the unburned flamelet and the last flamelet in Set #2. Because Set #2 burns more strongly than Set #3, the corresponding source terms are larger. This discussion highlights an interesting sensitivity of the non-premixed flamelet model that appears when the model is applied outside of the purely non-premixed regime. Moreover, no a-priori method exists of determining which flamelets are best for use in an arbitrary turbulent combustion simulation.

Two other important differences between the non-premixed FPV implementations and the finite rate solution can be noted in Figs. 3 and 4. The first is the nature of the computed solutions near the domain outlet at the middle time being considered (the second row in Fig. 3). Near this outlet, the finite rate solution is characterized by a strip of burned gas that extends upstream along the centerline. On either side of this centerline, pockets of relatively unburned gas exist. In the second FPV implementation, the strip of burned gas along the centerline is reasonably well represented, but the top half of the outlet consists primarily of burned gas. Conversely, in the third FPV implementation a pocket of unburned gas does exist along the top half of the outlet, but the gas along the centerline is primarily unburned. The implications of these differences are not immediately clear, and it is furthermore not clear which implementation can be said to be more accurate. What is clear, however, is that the particulars of the flamelet approach affect the computed flame structure.

The second notable difference appears in the CO species comparison shown in Fig. 4.

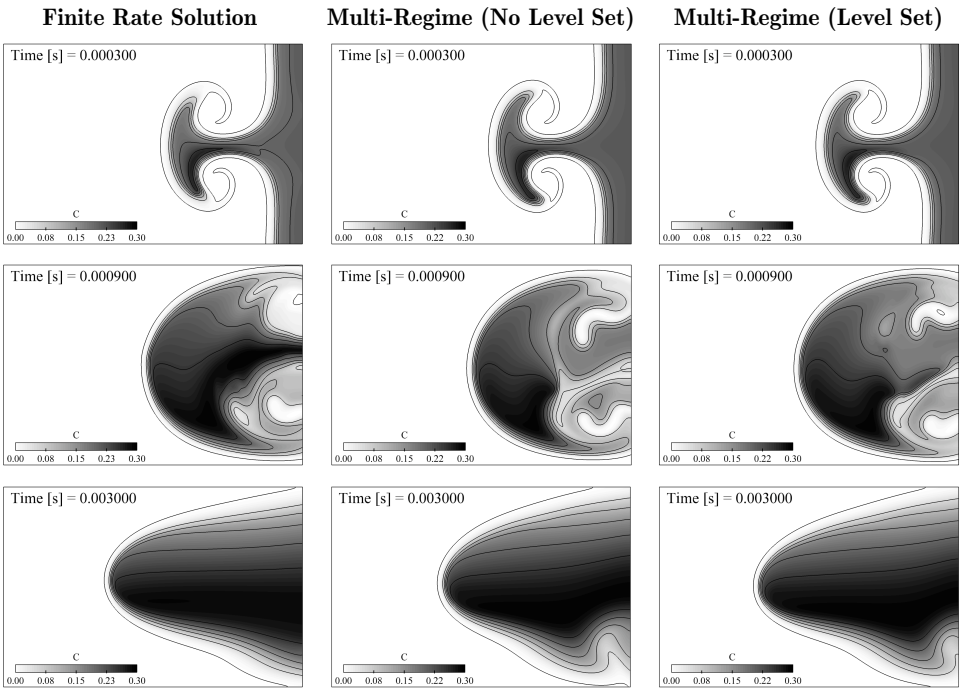

FIGURE 5. Progress variable fields in the triple flame, computed from the finite rate approach and from two multi-regime flamelet models.

In general, the FPV models tend to overpredict the amount of CO in the lean (top) half of the flame and underpredict the amount of CO in the rich (bottom) half of the flame. For example, in the first row of Fig. 4 the FPV models overpredict the CO mass fraction along the top half of the leading flame edge by approximately 20%. Similarly, in the third row of Fig. 4 the FPV models underpredict the amount of CO in the rich branch of the flame by as much as 45%. These incorrect predictions are partly due to the fact that the leading edge of the triple flame burns primarily in a premixed fashion. Because the CO concentrations that occur in non-premixed flamelets differ from the concentrations that occur in premixed flamelets, a certain amount of error is expected in the modeled CO fields. This error is clearly found in the simulations, and turns out to be significant in magnitude (20%-45%).

3.3. *Multi-regime flamelet model*

The multi-regime flamelet solutions are compared with the finite rate solution in Figs. 5 - 7. The first multi-regime model does not use a level set to describe the flame front; the second model does. Again, the first multi-regime model is designed to test the combined premixed and non-premixed flamelet approach in a concise fashion, whereas the second model tests a realizable LES implementation of the model. Similar to the second and third FPV implementations, these multi-regime models capture many of the features of the triple flame while remaining subject to certain errors. Significantly, the multi-regime models capture CO concentrations more accurately than the purely non-premixed models.

The multi-regime progress variable and density fields are shown in Figs. 5 and 6. Regardless of whether level set coupling is used, the multi-regime approach is able to

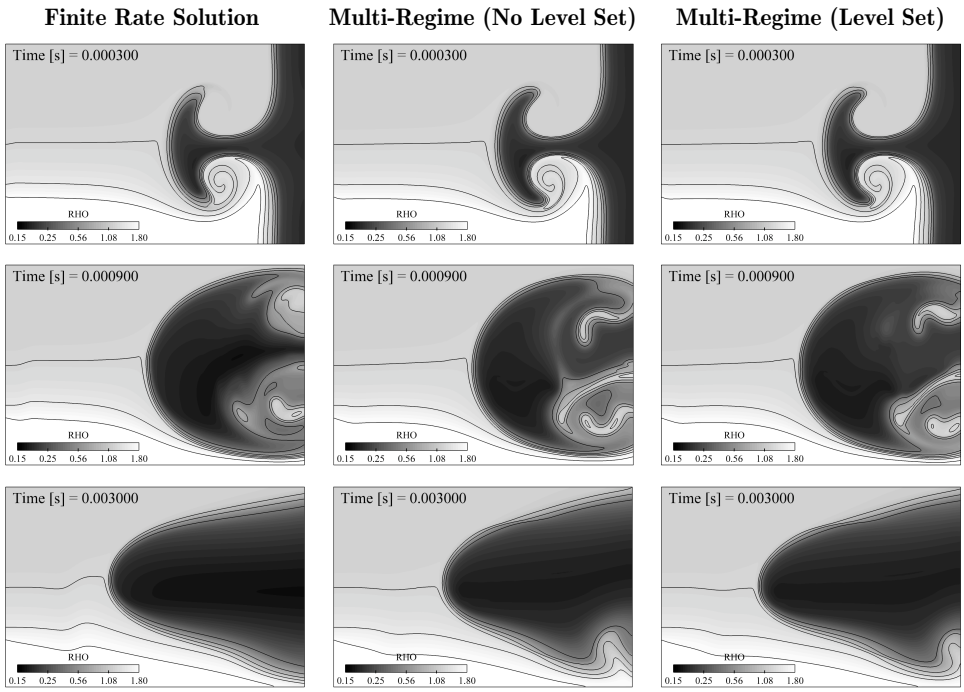

FIGURE 6. Density fields in the triple flame, computed from the finite rate approach and from two multi-regime flamelet models.

capture the location and structure of the leading flame edge reasonably well. In both multi-regime simulations, the predicted location of the leading edge at the last time being considered (third row of Fig. 5) is more accurate than in either of the non-premixed solutions (see Fig. 8 below). This is to a certain extent expected, since the leading edge is largely premixed and premixed flamelets better describe its behavior. Additionally, at the middle time being considered (second row of Fig. 5), the multi-regime approach correctly captures the existence of unburned regions at the domain outlet just above and below the centerline. The width and shape of these regions, however, is not in good agreement with the finite rate solution. This is especially noticeable in the lean (upper) half of the flame. Additionally, the model introduces a kink along the bottom of the flame profile at later times (third row in the figures). These discrepancies require further investigation in future work.

The CO concentrations predicted by the multi-regime models are shown in Fig. 7. In the top row of Fig. 7, the flamelet model is in excellent agreement with the finite rate solution. Both the structure and the magnitude of the CO field are predicted quite well. At later times, the minimum and maximum magnitudes of CO continue to be predicted well, but some errors do arise in predicted flame structure. In the middle set of plots, for example, the region of high CO concentration along the rich (bottom) side of the leading flame front is captured by the multi-regime model. In the finite rate solution, however, this region extends up toward the centerline and then downstream to the outlet, whereas in the multi-regime approach the high concentration diminishes around the centerline. Similarly, in the bottom set of plots the region of high CO concentration in the lower

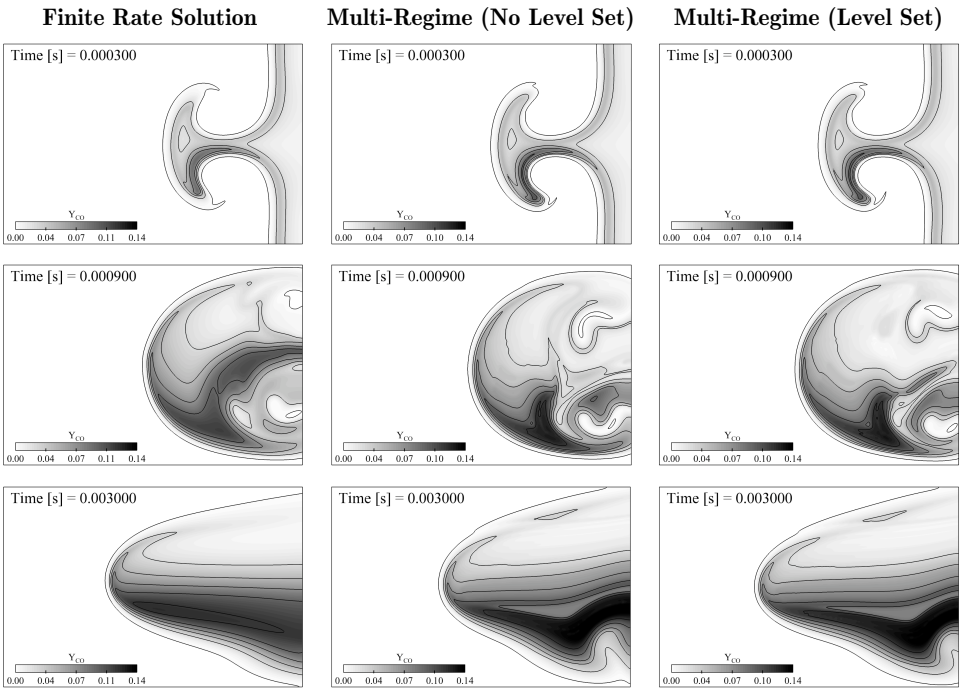

FIGURE 7. CO species fields in the triple flame, computed from the finite rate approach and from two multi-regime flamelet models.

half of the flame is accurately predicted by the flamelet model. The kink in the flame profile, however, distorts the agreement with the finite rate solution.

To compare the non-premixed and multi-regime flamelet models in a more quantitative sense, the location of the predicted leading flame edge is plotted as a function of time in Fig. 8 for four of the five model cases being considered. The leading flame edge location is defined as the horizontal coordinate in the computational domain where the progress variable first reaches a value of $C = 0.08$. During the initial stages of the simulation the two embedded vortices completely control the location of the leading flame edge, and the four models agree very well with the finite rate solution. As time advances, however, the modeled chemistry becomes more important and begins to control the leading edge location. Interestingly, Fig. 8 demonstrates that the two multi-regime flamelet models predict the leading edge's behavior with more accuracy than either of the non-premixed FPV models. Furthermore, the two FPV models are not consistent in the way that they induce error. Rather, one overpredicts the leading edge's propagation speed, while the other underpredicts it. This again emphasizes that the FPV approach is sensitive to the choice of which non-premixed flamelets are used for tabulation when deviations from the purely non-premixed regime occur.

The results in Fig. 8 indicate that premixed flamelet information is needed to correctly predict flame propagation in multi-regime settings. Once this has been recognized, it is interesting to note that the multi-regime model employing level set coupling predicts the flame propagation speed somewhat more accurately than the approach with no level set coupling. It is possible that the presence of the tabulated burning velocity $s_{L,u}$ in the level set equation accounts for the reaction and diffusion balance in the triple flame

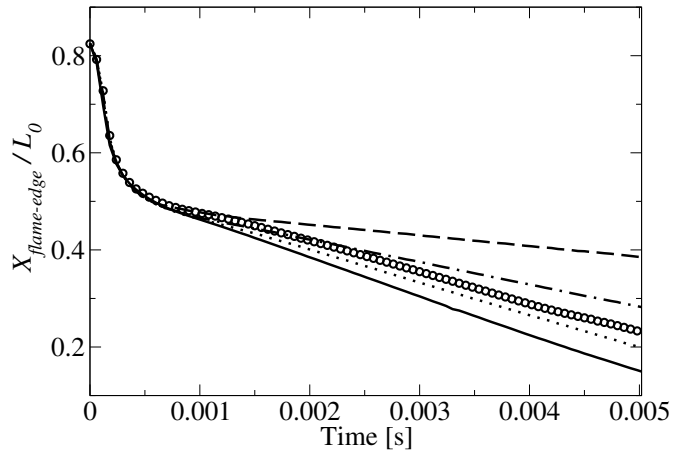

FIGURE 8. Location of the leading flame edge predicted by: Finite rate chemistry (○ ○ ○); FPV model, flamelet sets 1-2 (——); FPV model, flamelet sets 1-3 (– – –); Multi-Regime model, no level set (– · –); Multi-Regime model, level set coupling (· · ·). The flame location $X_{flame-edge}$ is normalized by the length of the computational domain, L_0.

better than does solving for the balance using the reduced progress variable coordinate's source term and diffusion coefficient. Further work on this topic, however, is required.

In summary, the multi-regime flamelet model tends to predict the evolution of the triple flame somewhat more accurately than the purely non-premixed approach. This is in part due to the fact that the location of the leading flame edge is more accurately predicted, and maybe even more significantly, in part due to the fact that the CO concentration is predicted with higher accuracy. In spite of this greater accuracy, a number of flame structure errors are still present in the multi-regime approach, and the predictions are not ideal.

4. Future work

Several open questions need to be more fully addressed before the triple flame that is considered here can be modeled with an acceptable degree of accuracy. Fortunately, many of these issues can be dealt with using currently available modeling infrastructure, such as the code and approach described in this work. In particular, future simulations and model development will focus on the following issues:

• The Smooth Combination Of Regimes. The effects associated with the current method of accessing and combining the different multi-regime databases were not addressed, but can strongly influence the quality of the density field in the simulation.

• Unsteadiness. The auto-ignition (unsteady) regime should be included in any fully regime-independent flamelet approach, and will be considered in the future.

• Larger Parameter Space. In addition to unsteadiness, effects such as radiation and heat losses should be tested by broadening the parameter space beyond the (Z,C) coordinates.

Acknowledgments

Support from the United States Air Force Office of Scientific Research (AFOSR) and from NASA is gratefully acknowledged.

REFERENCES

Colin, O., Ducros, F., Veynante, D. & Poinsot, T. 2000 A thickened flame model for large eddy simulations of turbulent premixed combustion. *Phys. Fluids*, **12**, 1843-1862.

Desjardins, O. Blanquart, G., Balarac, G. & Pitsch, H. 2007 High order conservative finite difference scheme for variable density low Mach number turbulent flows. *J. Comput. Phys.* **227**, 7125-7159.

Domingo, P., Vervisch, L. & Réveillon, J. 2005 DNS analysis of partially premixed combustion in spray and gaseous turbulent flame-bases stabilized in hot air. *Combust. Flame* **140**, 172-195.

Domingo, P., Vervisch, L. & Veynante, D. 2008 Large-eddy simulation of a lifted methane jet flame in a vitiated coflow. *Combust. Flame* **152**, 415-432.

Favier, V. & Vervisch, L. 2001 Edge flames and partially premixed combustion in diffusion flame quenching. *Combust. Flame* **125**, 788-803.

Ihme, M., Cha, C. M. & Pitsch, H. 2004 Prediction of local extinction and re-ignition effects in non-premixed turbulent combustion using a flamelet / progress variable approach. *Proc. Comb. Inst.* **30**, 793-800.

Liu, S., Hewson, J. C., Chen, J. H. & Pitsch, H. 2004 Effects of strain rate on high-pressure nonpremixed n-heptane autoignition in counterflow. *Combust. Flame* **137**, 320-339.

Knudsen, E. & Pitsch, H. 2009*a* A general flamelet transformation useful for distinguishing between premixed and non-premixed modes of combustion. *Combust. Flame* **156**, 678-696.

Knudsen, E. & Pitsch, H. 2009*b* An analysis of premixed flamelet models for large eddy simulation of turbulent combustion. *Phys. Fluids* Submitted.

Moureau, V., Fiorina, B. & Pitsch, H. 2009 A level set formulation for premixed combustion LES considering the turbulent flame structure. *Combust. Flame* **156**, 801-812.

Peters, N. 2000 *Turbulent Combustion.* Cambridge University Press, Cambridge, UK.

Pierce, C. D. & Moin, P. 2004 Progress-variable approach for large-eddy simulation of non-premixed turbulent combustion. *J. Fluid Mech.* **504**, 73-97.

Pitsch, H. & Peters, N. 1998 A consistent flamelet formulation for non-premixed combustion considering differential diffusion effects. *Combust. Flame* **114**, 26-40.

Pitsch, H. 1998 FlameMaster: A C++ computer program for 0D combustion and 1D laminar flame calculations. Available from http://www.stanford.edu/∼hpitsch/.

Pitsch, H. 2006 Large-eddy simulation of turbulent combustion. *Annu. Rev. Fluid Mech.* **38**, 453-483.

Yamashita, H., Shimada, M. & Takeno, T. 1996 A numerical study on flame stability at the transition point of jet diffusion flames. *Proc. Comb. Inst.* **26**, 27-34.